

## ON THE DETECTABILITY OF LIGHTCURVES OF KUIPER BELT OBJECTS

PEDRO LACERDA

Leiden Observatory, University of Leiden, Postbus 9513, NL-2300 RA Leiden, Netherlands

AND

JANE LUU

MIT Lincoln Laboratory, 244 Wood Street, Lexington, MA 02420, USA

Feb 2003

### ABSTRACT

We present a statistical study of the detectability of lightcurves of Kuiper Belt objects (KBOs). Some Kuiper Belt objects display lightcurves that appear "flat", i.e., there are no significant brightness variations within the photometric uncertainties. Under the assumption that KBO lightcurves are mainly due to shape, the lack of brightness variations may be due to (1) the objects have very nearly spherical shapes, or (2) their rotation axes coincide with the line of sight. We investigate the relative importance of these two effects and relate it to the observed fraction of "flat" lightcurves. This study suggests that the fraction of KBOs with detectable brightness variations may provide clues about the shape distribution of these objects. Although the current database of rotational properties of KBOs is still insufficient to draw any statistically meaningful conclusions, we expect that, with a larger dataset, this method will provide a useful test for candidate KBO shape distributions.

*Subject headings:* Kuiper Belt — minor planets, asteroids — solar system: general

### 1. INTRODUCTION

The Kuiper Belt holds a large population of small objects which are thought to be remnants of the protosolar nebula (Jewitt & Luu 1993). The Belt is also the most likely origin of other outer solar system objects such as Pluto-Charon, Triton, and the short-period comets; its study should therefore provide clues to the understanding of the processes that shaped our solar system. More than 650 Kuiper Belt objects (KBOs) are known to date and a total of about  $10^5$  objects larger than 50 km are thought to orbit the Sun beyond Neptune (Jewitt & Luu 2000).

One of the most fundamental ways to study physical properties of KBOs is through their lightcurves. Lightcurves show periodic brightness variations due to rotation, since, as the KBO rotates in space, its cross-section as projected in the plane of the sky will vary due to its non-spherical shape, resulting in periodic brightness variations (see Fig. 1). A well-sampled lightcurve will thus yield the rotation period of the KBO, and the lightcurve amplitude has information on the KBO's shape. This technique is commonly used in planetary astronomy, and has been developed extensively for the purpose of determining the shapes, internal density structures, rotational states, and surface properties of atmosphereless bodies. These properties in turn provide clues to their formation and collisional environment.

Although lightcurves studies have been carried out routinely for asteroids and planetary satellites, the number of KBO lightcurves is still meager, with few of sufficient quality for analysis (see Table 1). This is due to the fact that most KBOs are faint objects, with apparent red magnitude of  $m_R \sim 23$  (Trujillo *et al.* 2001), rendering it very difficult to detect small amplitude changes in their brightness. One of the few high qual-

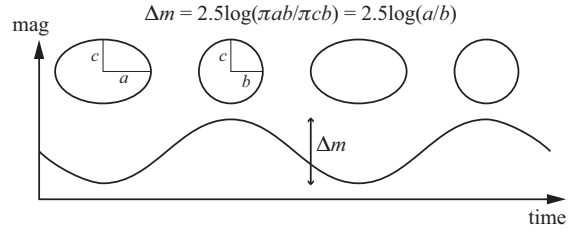


FIG. 1.— The lightcurve of an ellipsoidal KBO observed at aspect angle  $\theta = \pi/2$ . Cross-sections and lightcurve are represented for one full rotation of the KBO. The amplitude,  $\Delta m$ , of the lightcurve is determined for this particular case. See text for the general expression.

ity lightcurves is that of (20000) Varuna, which shows an amplitude of  $\Delta m = 0.42 \pm 0.02$  mag and a period of  $P_{\text{rot}} = 6.3442 \pm 0.0002$  hrs (Jewitt & Sheppard 2002). Only recently have surveys started to yield significant numbers of KBOs bright enough for detailed studies (Jewitt *et al.* 1998).

Another difficulty associated with the measurement of the amplitude of a lightcurve is the one of determining the period of the variation. If no periodicity is apparent in the data, any small variations in the brightness of an object must be due to noise. Furthermore, a precise measurement of the amplitude of the lightcurve requires a complete coverage of the rotational phase. Therefore, any conclusion based on amplitudes of lightcurves must assume that their periods have been determined and confirmed by well sampled phase plots of the data.

However, not all of the observed KBOs show detectable brightness variations (the so-called "flat" lightcurves). The simplest explanations for this could be due to (1) the object is axisymmetric (the two axes perpendicular to the spin vector are equal), or (2) its rotation axis is nearly coincident with the line of sight (see Fig. 3). In other words, the undetectable variations are either a con-

TABLE 1. KBOs WITH MEASURED LIGHTCURVES.

Name	Class <sup>a</sup>	$H$ <sup>b</sup> [mag]	$\Delta m$ <sup>c</sup> [mag]	$P$ <sup>d</sup> [hrs]	Source <sup>e</sup>
1993 SC	C	6.9	<0.04		RT99
1994 TB	P	7.1	0.3	6.5	RT99
1996 TL <sub>66</sub>	S	5.4	<0.06		RT99
1996 TP <sub>66</sub>	P	6.8	<0.12		RT99
1994 VK <sub>8</sub>	C	7.0	0.42	9.0	RT99
1996 TO <sub>66</sub>	C	4.5	0.1	6.25	Ha00
Varuna	C	3.7	0.42	6.34	JS02
1995 QY <sub>9</sub>	P	7.5	0.6	7.0	RT99
1996 RQ <sub>20</sub>	C	7.0	-		RT99
1996 TS <sub>66</sub>	C	6.4	<0.16		RT99
1996 TQ <sub>66</sub>	C	7.0	<0.22		RT99
1997 CS <sub>29</sub>	C	5.2	<0.2		RT99
1999 TD <sub>10</sub>	S	8.8	0.68	5.8	Co00

<sup>a</sup>dynamical class (C - classical KBO, P - plutino, S - scattered KBO)

<sup>b</sup>absolute magnitude

<sup>c</sup>lightcurve amplitude

<sup>d</sup>rotational period

<sup>e</sup>JS02 (Jewitt & Sheppard 2002), Ha00 (Hainaut 2000), Co00 (Consolmagno et al. 2000), RT99 (Romanishin & Tegler 1999)

TABLE 2. USED SYMBOLS AND NOTATION.

Symbol	Description
$a \geq b \geq c$	axes of ellipsoidal KBO
$\bar{a} \geq \bar{b} \geq \bar{c}$	normalized axes of KBO ( $\bar{b} = 1$ )
$\theta$	aspect angle
$\Delta m_{\min}$	minimum detectable lightcurve amplitude
$\theta_{\min}$	aspect angle at which $\Delta m = \Delta m_{\min}$
$K$	$10^{0.8\Delta m_{\min}}$

sequence of the KBO's shape, or of the observational geometry. By studying the relative probabilities of these two causes, and relating them to the observed fraction of "flat" lightcurves, we might expect to improve our knowledge of the intrinsic shape distribution of KBOs. In this paper we address the following question: Can we learn something about the shape distribution of KBOs from the fraction of "flat" lightcurves?

## 2. DEFINITIONS AND ASSUMPTIONS

The observed brightness variations in KBO lightcurves can be due to:

- eclipsing binary KBOs
- surface albedo variations
- irregular shape

In general the brightness variations will arise from some combination of these three factors, but the preponderance of each effect among KBOs is still not known. In the following calculations we exclude the first two factors and assume that shape is the sole origin of KBO brightness variations. We further assume that KBO shapes can be approximated by triaxial ellipsoids, and thus expect a typical KBO lightcurve to show a set of 2 maxima and 2 minima for each full rotation (see Fig. 1). Table 2 summarizes the used symbols and notations. The listed quantities are defined in the text.

The detailed assumptions of our model are as follows:

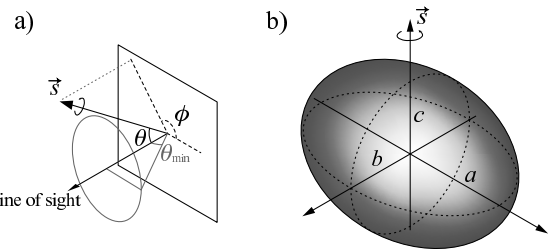


FIG. 2.— **a)** A spherical coordinate system is used to represent the observing geometry. The line of sight (oriented from the object to the observer) is the polar axis and the azimuthal axis is arbitrary in the plane orthogonal to the polar axis.  $\theta$  and  $\phi$  are the spherical angular coordinates of the spin axis  $\vec{s}$ . In this coordinate system the aspect angle is given by  $\theta$ . The "non-detectability" cone, with semi-vertical angle  $\theta_{\min}$ , is represented in grey. If the spin axis lies within this cone the brightness variations due to changing cross-section will be smaller than photometric errors, rendering it impossible to detect brightness variations. **b)** The picture represents an ellipsoidal KBO with axes  $a \geq b \geq c$ .

1. *The KBO shape is a triaxial ellipsoid.* This is the shape assumed by a rotating body in hydrostatic equilibrium (Chandrasekhar 1969). There are reasons to believe that KBOs might have a "rubble pile" structure (Farinella et al. 1981), justifying the approximation even further.
2. *The albedo is constant over surface.* Although albedo variegation can in principle explain any given lightcurve (Russell 1906), the large scale brightness variations are generally attributed to the object's irregular shape (Burns & Tedesco 1979).
3. *All axis orientations are equally probable.* Given that we have no knowledge of preferred spin vector orientation, this is the most reasonable *a priori* assumption.
4. *The KBO is in a state of simple rotation around the shortest axis (the axis of maximum moment of inertia).* This is likely since the damping timescale of a complex rotation (e.g., precession),  $\sim 10^3$  yr, (Burns & Safronov 1973), (Harris 1994) is smaller than the estimated time between collisions ( $10^7$ – $10^{11}$  yr) that would re-excite such a rotational state (Stern 1995), (Davis & Farinella 1997).
5. *The KBO is observed at zero phase angle ( $\alpha = 0$ )* It has been shown from asteroid data that lightcurve amplitudes seem to increase linearly with phase angle,

$$A(\theta, 0) = A(\theta, \alpha)/(1 + m\alpha) ,$$

where  $\theta$  is the aspect angle,  $\alpha$  is the phase angle and  $m$  is a coefficient which depends on surface composition. The aspect angle is defined as the angle between the line of sight and the spin axis of the KBO (see Fig. 2a), and the phase angle is the Sun-object-Earth angle. The mean values of  $m$  found for different asteroid classes are  $m(S) = 0.030$ ,  $m(C) = 0.015$ ,  $m(M) = 0.013$ , where S, C, and M are asteroid classes (Michalowsky 1993). Since KBO are distant objects the phase angle will always be small. Even allowing  $m$  to be one order

of magnitude higher than that of asteroids the increase in the lightcurve amplitude will not exceed 1%.

6. *The brightness of the KBO is proportional to its cross-section area (geometric scattering law).* This is a good approximation for KBOs because (1) most KBOs are too small to hold an atmosphere, and (2) the fact that they are observed at very small phase angles reduces the influence of scattering on the lightcurve amplitude (Magnusson 1989).

The KBOs will be represented by triaxial ellipsoids of axes  $a \geq b \geq c$  rotating around the short axis  $c$  (see Fig. 2b). In order to avoid any scaling factors we normalize all axes by  $b$ , thus obtaining a new set of parameters  $\bar{a}$ ,  $\bar{b}$  and  $\bar{c}$  given by

$$\bar{a} = a/b, \quad \bar{b} = 1, \quad \bar{c} = c/b. \quad (1)$$

As defined,  $\bar{a}$  and  $\bar{c}$  can assume values  $1 \leq \bar{a} < \infty$  and  $0 < \bar{c} \leq 1$ . Note that the parameters  $\bar{a}$  and  $\bar{c}$  are dimensionless.

The orientation of the spin axis of the KBO relative to the line of sight will be defined in spherical coordinates  $(\theta, \phi)$ , with the line of sight (oriented from the object to the observer) being the  $z$ -axis, or polar axis, and the angle  $\theta$  being the polar angle (see Fig. 2a). The solution is independent of the azimuthal angle  $\phi$ , which would be measured in the plane perpendicular to the line of sight, between an arbitrary direction and the projection of the spin axis on the same plane. The observation geometry is parameterized by the aspect angle, which in this coordinate system corresponds to  $\theta$ .

As the object rotates, its cross-section area  $S$  will vary periodically between  $S_{\max}$  and  $S_{\min}$  (see Fig. 1). These areas are simply a function of  $a$ ,  $b$ ,  $c$  and the aspect angle  $\theta$ . Given the assumption of geometric scattering, the ratio between maximum and minimum flux of reflected sunlight will be equal to the ratio between  $S_{\max}$  and  $S_{\min}$ . The lightcurve amplitude can then be calculated from the quantities  $\bar{a}$ ,  $\bar{c}$  and  $\theta$  and is given by

$$\Delta m = 2.5 \log \left( \frac{\bar{a}^2 \cos^2 \theta + \bar{a}^2 \bar{c}^2 \sin^2 \theta}{\bar{a}^2 \cos^2 \theta + \bar{c}^2 \sin^2 \theta} \right)^{1/2}. \quad (2)$$

### 3. “FLAT” LIGHTCURVES

It is clear from Eq. (2) that under certain conditions,  $\Delta m$  will be zero, i.e., the KBO will exhibit a flat lightcurve. These special conditions involve the shape of the object and the observation geometry, and are described quantitatively below. Taking into account photometric error bars will bring this “flatness” threshold to a finite value,  $\Delta m_{\min}$ , a minimum detectable amplitude below which brightness variation cannot be ascertained.

The two factors that influence the amplitude of a KBO lightcurve are:

**1. Sphericity** For a given ellipsoidal KBO of axes ratios  $\bar{a}$  and  $\bar{c}$  the lightcurve amplitude will be largest when  $\theta = \pi/2$  and smallest when  $\theta = 0$  or  $\pi$ . At  $\theta = \pi/2$ , Eq. (2) becomes

$$\Delta m = 2.5 \log \bar{a}. \quad (3)$$

Even at  $\theta = \pi/2$ , having a minimum detectable amplitude,  $\Delta m_{\min}$ , puts constraints on  $\bar{a}$  since if  $\bar{a}$  is too small,

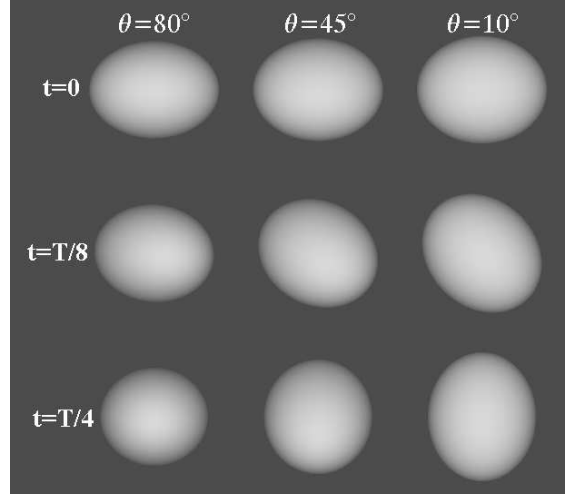


FIG. 3.— Illustration of a rotating ellipsoid at different aspect angles. A quarter of a full rotation is represented. Rotational phase of ellipsoid increasing from top to bottom and  $\theta$  decreasing from left to right.  $T$  is the period of rotation. Axes ratios are  $\bar{a} = 1.2$  and  $\bar{c} = 0.9$ .

the lightcurve amplitude will not be detected. This constraint is thus

$$\bar{a} < 10^{0.4\Delta m_{\min}} \Rightarrow \text{“flat” lightcurve}. \quad (4)$$

**2. Observation geometry** If the rotation axis is nearly aligned with the line of sight, i.e., if the aspect angle is sufficiently small, the object’s projected cross-section will hardly change with rotation, yielding no detectable brightness variations (see Fig. 3). The finite accuracy of the photometry defines a minimum aspect angle,  $\theta_{\min}$ , within which the lightcurve will appear flat within the uncertainties. This angle rotated around the line of sight generates the “non-detectability cone” (see Fig. 2a), with the solid angle

$$\Omega(\theta_{\min}) = \int_0^{2\pi} \int_0^{\theta_{\min}} \sin \theta \, d\theta \, d\phi. \quad (5)$$

Any aspect angle  $\theta$  which satisfies  $\theta < \theta_{\min}$  falls within the “non-detectability cone” and results in a non-detectable lightcurve amplitude. Therefore, the probability that the lightcurve will be flat due to observing geometry is

$$p_{\bar{a}, \bar{c}}(\text{non-detection}) = \frac{2 \times \Omega(\theta_{\min})}{4\pi} = 1 - \cos \theta_{\min} \quad (6a)$$

$$p_{\bar{a}, \bar{c}}(\text{detection}) = \cos \theta_{\min}. \quad (6b)$$

The factor of 2 accounts for the fact that the axis might be pointing towards or away from the observer and still give rise to the same observations, and the  $4\pi$  in the denominator represents all possible axis orientations.

From Eq. (2) we can write  $\cos \theta_{\min}$  as a function of  $\bar{a}$  and  $\bar{c}$ ,

$$\cos \theta_{\min} = \Psi(\bar{a}, \bar{c}) = \sqrt{\frac{\bar{c}^2(\bar{a}^2 - K)}{\bar{c}^2(\bar{a}^2 - K) + \bar{a}^2(K - 1)}}, \quad (7)$$

where  $K = 10^{0.8\Delta m_{\min}}$ . The function  $\Psi(\bar{a}, \bar{c})$ , represented in Fig. 4, is the probability of detecting brightness variation from a given ellipsoid of axes ratios  $(\bar{a}, \bar{c})$ .

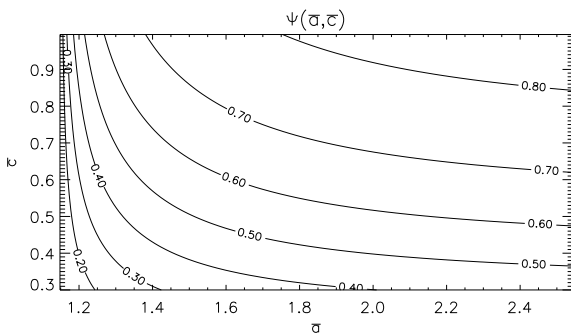


FIG. 4.— The function  $\Psi(\bar{a}, \bar{c})$  (Eq. (7)). This plot assumes photometric errors  $\Delta m_{\min} = 0.15$  mag. The detection probability is zero when  $\bar{a} < 10^{0.4\Delta m_{\min}} \approx 1.15$ .

It is a geometry weighting function. For  $\bar{a}$  in  $[1, \sqrt{K}]$  we have  $\Psi(\bar{a}, \bar{c}) = 0$  by definition, since in this case the KBO satisfies Eq. (4) and its lightcurve amplitude will not be detected irrespective of the aspect angle. It is clear from Fig. 4 that it is more likely to detect brightness variation from an elongated body.

#### 4. DETECTABILITY OF LIGHTCURVES

In order to generate a “non-flat” lightcurve, the KBO has to satisfy both the shape and observation geometry conditions. Mathematically this means that the probability of detecting brightness variation from a KBO is a function of the probabilities of the KBO satisfying both the sphericity and observing geometry conditions.

We will assume that it is possible to represent the shape distribution of KBOs by two independent probability density functions,  $f(\bar{a})$  and  $g(\bar{c})$ , defined as

$$p(\bar{a}_1 \leq \bar{a} \leq \bar{a}_2) = \int_{\bar{a}_1}^{\bar{a}_2} f(\bar{a}) d\bar{a}, \int_1^\infty f(\bar{a}) d\bar{a} = 1, \quad (8a)$$

$$p(\bar{c}_1 \leq \bar{c} \leq \bar{c}_2) = \int_{\bar{c}_1}^{\bar{c}_2} g(\bar{c}) d\bar{c}, \int_0^1 g(\bar{c}) d\bar{c} = 1, \quad (8b)$$

where the integrals on the left represent the fraction of KBOs in the given ranges of axes ratios. This allows us to write the following expression for  $p(\Delta m > \Delta m_{\min})$ , where both the shape and observation geometry constraints are taken into account,

$$p(\Delta m > \Delta m_{\min}) = \int_0^1 \int_1^\infty \Psi(\bar{a}, \bar{c}) f(\bar{a}) g(\bar{c}) d\bar{a} d\bar{c}. \quad (9)$$

The right hand side of this equation represents the probability of observing a given KBO with axes ratios between  $(\bar{a}, \bar{c})$  and  $(\bar{a} + d\bar{a}, \bar{c} + d\bar{c})$ , at a large enough aspect angle, integrated for all possible axes ratios. This is also the probability of detecting brightness variation for an observed KBO.

The lower limit of integration for  $\bar{a}$  in Eq. (9) can be replaced by  $\sqrt{K}$ , with  $K$  defined as in Eq. (7), since  $\Psi(\bar{a}, \bar{c})$  is zero for  $\bar{a}$  in  $[1, \sqrt{K}]$ . In fact, this is how the sphericity constraint is taken into account.

Provided that we know the value of  $p(\Delta m > \Delta m_{\min})$  Eq. (9) can test candidate distributions  $f(\bar{a})$  and  $g(\bar{c})$  for the shape distribution of KBOs. The best estimate for  $p(\Delta m > \Delta m_{\min})$  is given by the ratio of “non-flat” lightcurves ( $N_D$ ) to the total number of measured lightcurves ( $N$ ), i.e.,

$$p(\Delta m > \Delta m_{\min}) \approx \frac{N_D}{N}. \quad (10)$$

Because  $N$  is not the total number of KBOs there will be an error associated with this estimate. Since we do not know the distributions  $f(\bar{a})$  and  $g(\bar{c})$  we will assume that the outcome of an observation can be described by a binomial distribution of probability  $p(\Delta m > \Delta m_{\min})$ . This is a good approximation given that  $N$  is very small compared with the total number of KBOs. Strictly speaking, the hypergeometric distribution should be used since we will not unintentionally observe the same object more than once (sampling without replacement). However, since the total number of KBOs (which is not known with certainty) is much larger than any sample of lightcurves, any effects of repeated sampling will be negligible, thereby justifying the binomial approximation. This simplification allows us to calculate the upper ( $p_+$ ) and lower ( $p_-$ ) limits for  $p(\Delta m > \Delta m_{\min})$  at any given confidence level,  $C$ . These values, known as the Clopper-Pearson confidence limits, can be found solving the following equations by trial and error (Barlow 1989),

$$\sum_{r=N_D+1}^N P(r; p_+(\Delta m > \Delta m_{\min}), N) = \frac{C+1}{2} \quad (11a)$$

$$\sum_{r=0}^{N_D-1} P(r; p_-(\Delta m > \Delta m_{\min}), N) = \frac{C+1}{2}, \quad (11b)$$

(see Table 2 for notation) where  $C$  is the desired confidence level and  $P(r; p, N)$  is the binomial probability of detecting  $r$  lightcurves out of  $N$  observations, each lightcurve having a detection probability  $p$ . Using the values in Table 1 and  $\Delta m_{\min} = 0.15$  mag we have  $N_D = 5$  and  $N = 13$  which yields  $p(\Delta m > \Delta m_{\min}) = 0.38^{+0.18}_{-0.15}$  at a  $C = 0.68$  ( $1\sigma$ ) confidence level. At  $C = 0.997$  ( $3\sigma$ ) we have  $p(\Delta m > \Delta m_{\min}) = 0.38^{+0.41}_{-0.31}$ . The value of  $p(\Delta m > \Delta m_{\min})$  could be smaller since some of the flat lightcurves might not have been published.

Note that for moderately elongated ellipsoids (small  $\bar{a}$ ) the function  $\Psi(\bar{a}, \bar{c})$  is almost insensitive to the parameter  $\bar{c}$  (see Fig. 4), in which case the axisymmetric approximation with respect to  $\bar{a}$  can be made yielding  $\bar{c} \approx 1$ . Eq. (9) then has only one unknown parameter,  $f(\bar{a})$ .

$$p(\Delta m > \Delta m_{\min}) \approx \int_{\sqrt{K}}^{\bar{a}_{\max}} \Psi(\bar{a}, 1) f(\bar{a}) d\bar{a} \approx 0.38^{+0.41}_{-0.31}. \quad (12)$$

If we assume the function  $f(\bar{a})$  to be gaussian, we can use Eq. (12) to determine its mean  $\mu$  and standard deviation  $\sigma$ , after proper normalization to satisfy Eq. (8a). The result is represented in Fig. 5, where we show all possible pairs of  $(\mu, \sigma)$  that would satisfy a given  $p(\Delta m > \Delta m_{\min})$ . For example, the line labeled “0.38” identifies all possible pairs of  $(\mu, \sigma)$  that give rise to  $p(\Delta m >$

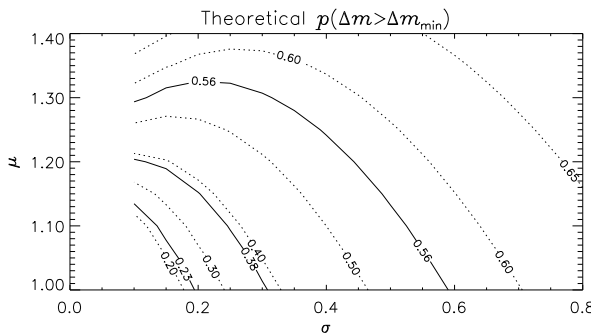


FIG. 5.— Contour plot of the theoretical probabilities of detecting brightness variation in KBOs (assuming  $\Delta m_{\min} = 0.15$  mag), drawn from gaussian shape distributions parameterized by  $\mu$  and  $\sigma$  (respectively the mean and spread of the distributions). The solid lines represent the observed ratio of “non-flat” lightcurves (at 0.38 and 0.68 confidence limits (at 0.23 and 0.56 respectively).

$\Delta m_{\min}$ ) = 0.38, the line labeled ”0.56” all possible pairs of  $(\mu, \sigma)$  that give rise to  $p(\Delta m > \Delta m_{\min}) = 0.56$ , etc.

Clearly, with the present number of lightcurves the uncertainties are too large to draw any relevant conclusions on the shape distribution of KBOs. With a larger dataset, this formulation will allow us to compare the distribution of KBO shapes with that of the main belt asteroids. The latter has been shown to resemble, to some extent, that of fragments of high-velocity impacts (Catullo *et al.* 1984). It deviates at large asteroid sizes that have presumably relaxed to equilibrium figures. A comparison of  $f(\bar{a})$  with asteroidal shapes should tell us, at the very least, whether KBO shapes are collisionally derived, as opposed to being accretional products.

The usefulness of this method is that, with more data, it would allow us to derive such quantitative parameters as the mean and standard deviation of the KBO shape distribution, if we assume *a priori* some intrinsic form for this distribution. The method’s strength is that it relies solely on the detectability of lightcurve amplitudes, which is more robust than other lightcurve parameters.

This paper focuses on the influence of the observation geometry and KBO shapes in the results of lightcurve measurements. In which direction would our conclusions change with the inclusion of albedo variegation and/or binary KBOs?

Non-uniform albedo would cause nearly spherical KBOs to generate detectable brightness variations, depending on the coordinates of the albedo patches on the KBO’s surface. This means that our method would overestimate the number of elongated objects by attributing all brightness fluctuations to asphericity.

Binary KBOs would influence the results in different ways depending on the orientation of the binary system’s orbital plane, on the size ratio of the components, and on the individual shapes and spin axis orientations of the primary and secondary. For example, an elongated KBO observed equator-on would have its lightcurve flattened by a nearly spherical moon orbiting in the plane of the sky, whereas two spherical KBOs orbiting each other would generate a lightcurve if the binary would be observed edge-on.

These effects are not straightforward to quantify analytically and might require a different approach. We intend to incorporate them in a future study. Also, with a larger sample of lightcurves it would be useful to apply this model to subgroups of KBOs based on dynamics, size, etc.

## 5. CONCLUSIONS

We derived an expression for the probability of detecting brightness variations from an ellipsoidal KBO, as a function of its shape and minimum detectable amplitude. This expression takes into account the probability that a “flat” lightcurve is caused by observing geometry.

Our model can yield such quantitative parameters as the mean and standard deviation of the KBO shape distribution, if we assume *a priori* an intrinsic form for this distribution. It concerns solely the statistical probability of detecting brightness variation from objects drawn from these distributions, given a minimum detectable lightcurve amplitude. The method relies on the assumption that albedo variegation and eclipsing binaries play a secondary role in the detection of KBO lightcurves. The effect of disregarding albedo variegation in our model is that we might overestimate the fraction of elongated objects. Binaries in turn could influence the result in both directions depending on the geometry of the problem, and on the physical properties of the constituents. We intend to incorporate these effects in a future, more detailed study.

We are grateful to Garrett Mellem, Glenn van de Ven, and Prof. John Rice for helpful discussion.

## REFERENCES

Barlow, R. 1989. Statistics. A guide to the use of statistical methods in the physical sciences. The Manchester Physics Series, New York: Wiley, 1989.

Burns, J. A. and V. S. Safronov 1973. Asteroid nutation angles. *MNRAS* 165, 403-411.

Burns, J. A. and E. F. Tedesco 1979. Asteroid lightcurves - Results for rotations and shapes. *Asteroids* 494-527.

Catullo, V., V. Zappalà, P. Farinella, and P. Paolicchi 1984. Analysis of the shape distribution of asteroids. *A&A* 138, 464-468.

Chandrasekhar, S. 1987. Ellipsoidal figures of equilibrium. New York : Dover, 1987..

Consolmagno, G. J., S. C. Tegler, T. Rettig, and W. Romanishin 2000. Size, Shape, Rotation, and Color of the Outer Solar System Object 1999 TD10. *AAS/Division for Planetary Sciences Meeting* 32, 21.07.

Davis, D. R. and P. Farinella 1997. Collisional Evolution of Edgeworth-Kuiper Belt Objects. *Icarus* 125, 50-60.

Farinella, P., P. Paolicchi, E. F. Tedesco, and V. Zappalà 1981. Triaxial equilibrium ellipsoids among the asteroids. *Icarus* 46, 114-123.

Hainaut, O. R., C. E. Delahodde, H. Boehnhardt, E. Dotto, M. A. Barucci K. J. Meech, J. M. Bauer, R. M. West, and A. Doressoundiram 2000. Physical properties of TNO 1996 TO<sub>66</sub>. Lightcurves and possible cometary activity. *A&A* 356, 1076-1088.

Harris, A. W. 1994. Tumbling asteroids. *Icarus* 107, 209.

Jewitt, D. and J. Luu 1993. Discovery of the candidate Kuiper belt object 1992 QB1. *Nature* 362, 730-732.

Jewitt, D., J. Luu, and C. Trujillo 1998. Large Kuiper Belt Objects: The Mauna Kea 8K CCD Survey. *AJ* 115, 2125-2135.

Jewitt, D. C. and J. X. Luu 2000. Physical Nature of the Kuiper Belt. *Protostars and Planets IV* 1201.

Jewitt, D. C. and S. S. Sheppard 2002. Physical Properties of Trans-Neptunian Object (20000) Varuna. *AJ* 123, 2110-2120.

Magnusson, P. 1989. Pole determinations of asteroids. *Asteroids II* 1180-1190.

Michalowski, T. 1993. Poles, shapes, senses of rotation, and sidereal periods of asteroids. *Icarus* 106, 563.

Romanishin, W. and S. C. Tegler 1999. Rotation rates of Kuiper-belt objects from their light curves. *Nature* 398, 129-132.

Russell, H. N. 1906. On the light variations of asteroids and satellites. *ApJ* 24, 1-18.

Stern, S. A. 1995. Collisional Time Scales in the Kuiper Disk and Their Implications. *AJ* 110, 856.

Trujillo, C. A., J. X. Luu, A. S. Bosh, and J. L. Elliot 2001. Large Bodies in the Kuiper Belt. *AJ* 122, 2740-2748.